

Study on thermal properties of TBAB–THF hydrate mixture for cold storage by DSC

Gang Li · Daoping Liu · Yingming Xie

Received: 7 February 2010/Accepted: 1 April 2010/Published online: 16 April 2010
© Akadémiai Kiadó, Budapest, Hungary 2010

Abstract In order to study the thermal properties of new type environment-friendly binary hydrate for cold storage in air-conditioning system, tests have been carried out by DSC comprehensively on the phase-change temperature and fusion heat of TBAB hydrate, THF hydrate, and TBAB–THF hydrate mixture. The results show a good trend that TBAB–THF hydrate has the superiority for more proper phase-change temperature and increased fusion heat. A broader and more developed view is that adding appropriate amount of hydrate with lower phase-change temperature to hydrate with higher one can make the hydrate mixture more suitable for cold storage (especially for 278–281 K); some hydrates with lower phase-change temperature can even make the fusion heat of mixture hydrate increased greatly. Several new environmental working pairs for binary gas hydrates have been listed to help to promote the application.

Keywords TBAB–THF hydrate mixture · DSC · Cold storage · Fusion heat

Introduction

Recently, the increasing demand of electric power for residential air conditioning has been more urgent in many countries [1–3]. The hydrate cold storage system, which can shift the demand to off-peak period and contribute to the load leveling of power generation, has been developed

commonly as the suitable new-type energy-saving system for its larger cold storage density and higher chiller efficiency compared to other storage systems (i.e., water, ice, eutectic salt storage system, etc.) [4, 5]. The refrigerant's gas hydrates, usually formed above 273.15 K and under moderate pressure, formation heat of which is comparable to the fusion heat of ice, can be considered as promising energy storage materials in air-conditioning systems [6–12]. Gas hydrates, also called gas clathrates, which are ice-like structures composed by a host lattice consisting of hydrogen-bounded water molecules that host small gaseous molecules [13, 14], have also widely been applied in storage and transportation of natural gas [15–17], separation of gas mixtures [18], CO₂ sequestration [19–22], sea water desalination [23], etc.

The thermal properties for hydrates, mainly about phase-change temperature and fusion heat (i.e., enthalpy of dissociation), which can be obtained by the innovative, rapid, and sensitive technology—differential scanning calorimetry (DSC) [24–28], are essentially important for cold storage system for air conditioning both with suitable temperature (278–281 K) and higher latent heat. However, still few new-type effective environment-friendly gas hydrates have been studied to repair the ozone shield and halt the greenhouse effect in air-conditioning cold storage system according to the Montreal Protocol on Substances that Deplete the Ozone Layer 2007 [29]. To the single hydrate, xenon, krypton, ethylene oxide, CH₄, C₃H₈ hydrates, etc., were tested by DSC by early researchers [30–33] and have been summarized reasonably and thoroughly by Sloan and Carolyn [14] later. However, they are hampered in air conditioning for cold storage by their harsh high-pressure conditions. HCFC-141b hydrate has been studied with DSC [34] and proved to be potential for cold storage these years, but it has been destined to be

G. Li (✉) · D. Liu · Y. Xie
School of Energy & Power Engineering, University of Shanghai
for Science and Technology, No. 516 Jun Gong RD,
Shanghai 200093, People's Republic of China
e-mail: gangli166@gmail.com

eliminated for its damage to the ozone layer. With regard to the mixture, TBAB hydrates with N₂, CO₂, N₂ + CO₂, CH₄ + CO₂, etc. have been studied [35, 36], but the phase-change temperatures are beyond the range for air-conditioning system. In addition, more attention has been paid to natural gas hydrates in the system containing salt [37–40], which are not for the field of cold storage. Obviously, still not much interest has been spawned to provide a wealth of ideas regarding their significance in air conditioning.

In this study, alternative refrigerants tetra-*n*-butyl ammonium bromide (TBAB) hydrate, tetrahydrofuran (THF) hydrate, and their mixture TBAB–THF hydrate have been selected for cold storage materials. Recently, researchers have merely studied the TBAB hydrates from the aspects of structure [41], phase equilibrium [42], interfacial kinetics [43], and flow behavior [44]; even though heats of fusion of TBAB have been tested by the relatively new DSC [45], much work still has to be carried out for mixture hydrate, which has more potential and superiority for practical applications. In this study, the phase-change temperature and fusion heat of TBAB hydrate, THF hydrate, and TBAB–THF hydrate mixture have been investigated by DSC and analyzed reasonably to provide several perspectives for application for cold storage in air-conditioning system.

Experimental procedure

Sample preparation

Hydrate samples were all made under 273.6 K and atmospheric pressure. In these cases, TBAB hydrate were prepared by mixing TBAB and water in the mole ratio 1/17, and THF hydrate also in the ratio 1/17. With regard to TBAB–THF hydrate mixture, TBAB, THF, and water were in the mole ratio 0.1/0.9/15, 0.3/0.7/15 for two samples. All the samples were prepared in a stirred vessel under laboratory conditions and preserved in refrigerator under proper low temperatures about 263 K; after all, the high-quality of samples were hard to obtain even at 273 K proved by plentiful tests for the disturbance of higher and unstable room temperature and other factors [36]. Also due to the hydrate poor stability at room conditions, the exact mass determination of the hydrate samples had to be made as soon as possible; in fact, both weighing and transferring them to DSC instrument took a longer time, which may make part of the samples for dehydrate [36]. Accordingly, samples must be prepared carefully and quickly. HCFC-141b hydrate, with HCFC-141b and water in the mole ratio 1/17, had also been made as the cold storage material for reliability verification of experimental apparatus. Freshly distilled and degassed water was offered to prepare all the

solutions. The mass of the sample used was determined with an electronic mass comparator—TG332a with a precision of ± 0.01 mg and range of 0–20 g.

DSC device and procedure

As can be seen from Figs. 1 and 2, all tests were performed on a DSC-Pyris Diamond type with advanced thermal analysis software—Pyris Software 5.0, which was produced by the company of Perkin–Elmer from the United States. Precision for thermal analysis is $\pm 0.1\%$, precision for recorded temperature is $\pm 0.01\%$, and the dynamic range for thermal analysis is 0.2 μW –800 mW.

With respect to the sample, crystallization in DSC experiments always requires that a certain subcooling should be needed and reached to compensate for the absence of agitation, and a refrigerating cooling system was used with a flow rate of 20 mL min⁻¹ of nitrogen with purity of 99.99%. The instrument was calibrated for the temperature at cooling and heating scanning rates of 2 and 1 K min⁻¹, respectively. The range of room temperature was 281–288 K. By the setting of proper programmed temperature and heating power, the thermal properties of samples could be investigated and analyzed reasonably by Pyris Software 5.0 of DSC.

The procedure for DSC is listed as follows:

- (1) Sensitivity calibration, temperature calibration, and furnace calibration were needed to ensure the temperature accuracy for tests.
- (2) Then, the preliminarily reliability for the apparatus was verified with materials (ice, indium).
- (3) HCFC-141b hydrate was tested by DSC for further reliability verification of apparatus for other new hydrates.
- (4) Samples—TBAB hydrate, THF hydrate, and TBAB–THF hydrate were tested and analyzed for confirming their feasibility for cold storage in air-conditioning system.

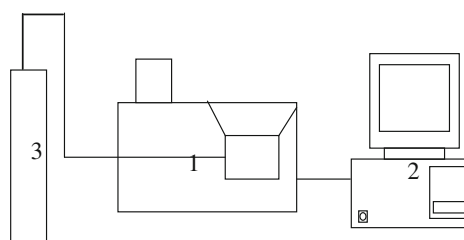


Fig. 1 Schematic diagram of the experimental apparatus of DSC. 1 Differential thermal analysis—Pyris Diamond; 2 micro-computer control and data acquisition system; and 3 high-purity nitrogen bottle



Fig. 2 Appearance and interior part of the furnace body of DSC—Pyris Diamond

Results and discussion

DSC curves of pure ice and indium

The DSC curves of pure ice and indium are shown in Figs. 3 and 4. Only one melting endothermic peak in the reversing heat flow curve for only the single substance (ice or indium) under the process of melting by DSC. According to the thermal analysis software, phase-change temperature (t_m) is the corresponding point (*onset*), which is the intersection of the tangent of endothermic curve and standard baseline connecting two endpoints for the endothermic peak. The fusion heat (ΔH) is shown in figures.

The thermal properties (phase-change temperature, fusion heat) of ice investigated and analyzed by DSC are (272.98 K, $338.80 \text{ kJ kg}^{-1}$). Compared with the standard value (273.15 K, 335 kJ kg^{-1}) [46] of ice, the deviation for temperature is only 0.17 K, and the deviation rate for fusion heat is 1.1%; obviously, the apparatus is reliable with DSC for thermal analysis.

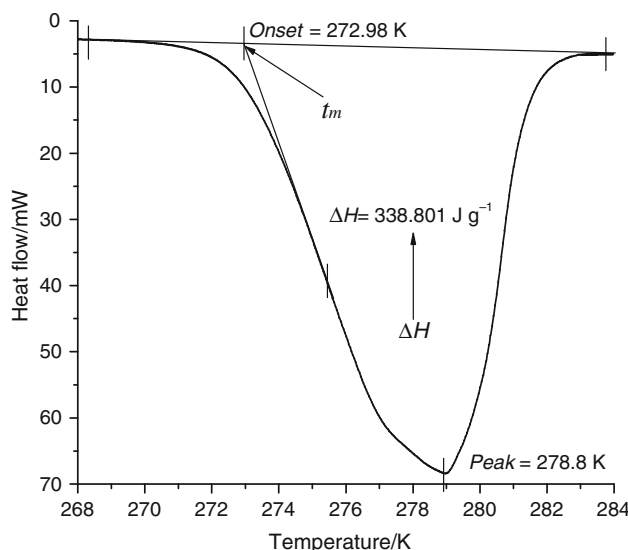


Fig. 3 DSC melting curve of ice, $m_{\text{ice}} = 12.54 \text{ mg}$

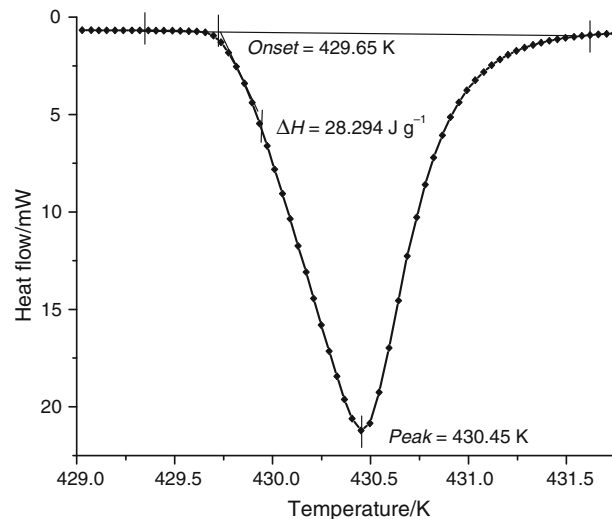


Fig. 4 DSC melting curve of indium, $m_{\text{indium}} = 5.74 \text{ mg}$

Similarly, the thermal properties of indium are (429.65 K, 28.29 kJ kg^{-1}). Compared with the standard value (429.81 K, 28.41 kJ kg^{-1}) [46], the deviation for temperature is only 0.16 K, and the deviation rate for fusion heat is 0.4%; the same conclusion can be drawn based on the thermal analysis.

DSC curves of HCFC-141b hydrate, TBAB hydrate, and THF hydrate

The DSC curves of HCFC-141b hydrate, TBAB hydrate, and THF hydrate are given in Figs. 5, 6, 7, and 8. Differently, two melting endothermic peaks in the reversing heat flow curve in these figures since there are two substances (ice and HCFC-141b, or TBAB, or THF). With regard to the first, the ice made with the help of super cooling occurs first, at a temperature which is slightly decreasing with pressure raise, according to the usual water melting point versus pressure law. Then, a second peak occurs, at a temperature which is strongly pressure-dependent. We attributed this peak to hydrate dissociation and took the second-onset temperature as phase-change temperature for hydrates (t_m). It should be noticed that, because of the existence of ice, the fusion heat $\Delta H_{\text{gas}1}$ shown in the figures are not the real value $-\Delta H_{\text{gas}}$; in order to get ΔH_{gas} , the part of fusion heat made by ice must be removed.

The ΔH_{gas} is calculated using the equation:

$$\begin{aligned}\Delta H_{\text{gas}} &= \Delta H_{\text{gas}1} \times m_{\text{total}} / (m_{\text{total}} - \Delta H_{\text{ice}1} \times m_{\text{total}} / \Delta H_{\text{ice}}) \\ &= \Delta H_{\text{gas}1} / (1 - \Delta H_{\text{ice}1} / \Delta H_{\text{ice}}),\end{aligned}\quad (1)$$

where $m_{\text{total}}/\text{mg}$ is mass of total hydrate sample; $\Delta H_{\text{gas}1}/\text{kJ kg}^{-1}$, nominal fusion heat for hydrate shown in the figures; $\Delta H_{\text{gas}}/\text{kJ kg}^{-1}$, real fusion heat for hydrate; $\Delta H_{\text{ice}1}/\text{kJ kg}^{-1}$, fusion heat for ice.

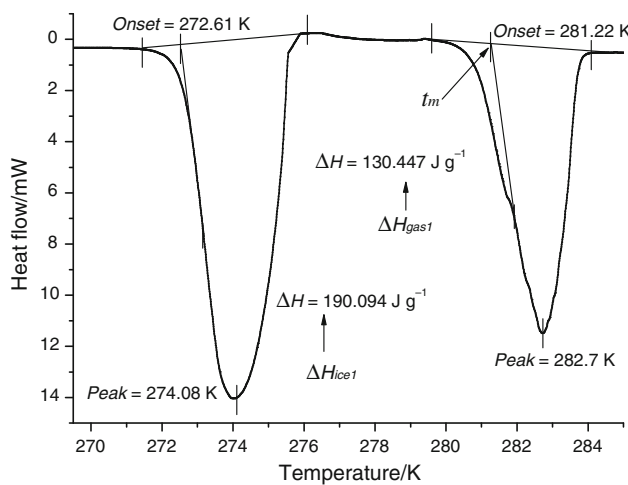


Fig. 5 DSC melting curve of HCFC-141b hydrate (1)

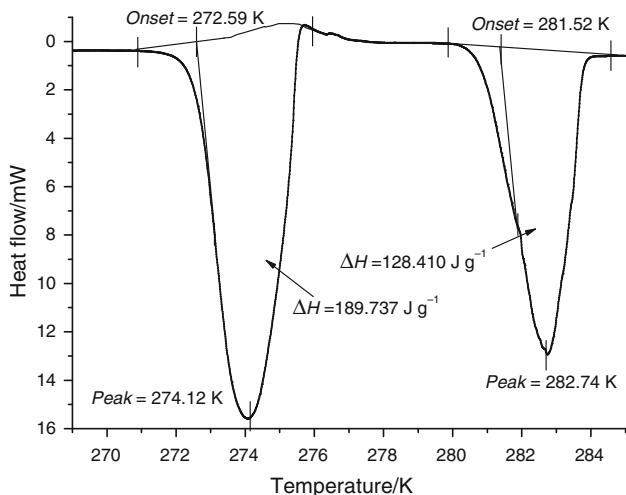


Fig. 6 DSC melting curve of HCFC-141b hydrate (2)

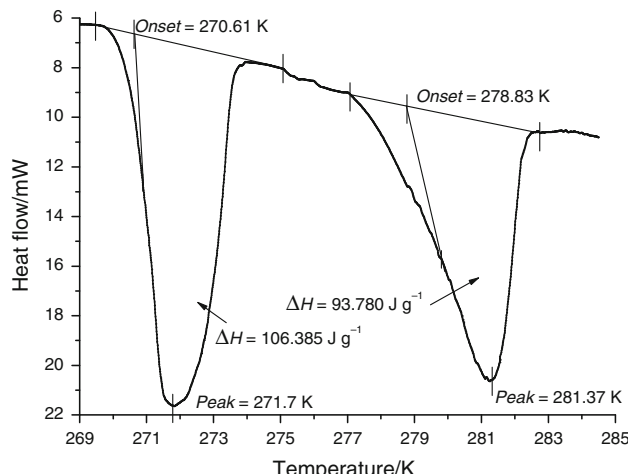


Fig. 7 DSC melting curve of TBAB hydrate

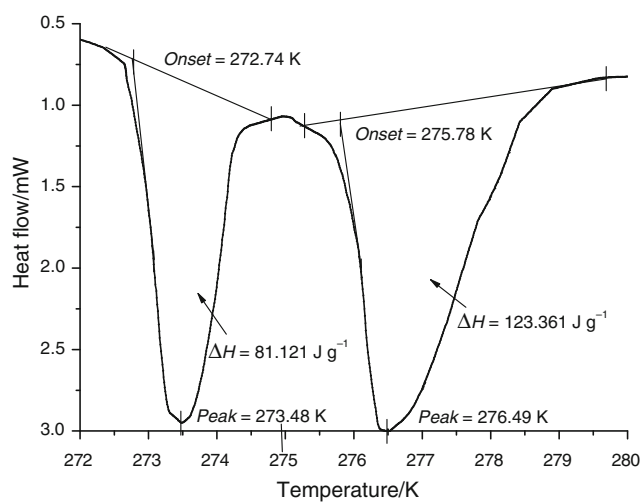


Fig. 8 DSC melting curve of THF hydrate

Table 1 Analysis of the thermal property of single gas hydrate

Sample	HCFC-141b hydrate (1)	HCFC-141b hydrate (2)	TBAB hydrate	THF hydrate
m_{total}/mg	10.10	9.58	15.93	10.28
t_m/K	281.2	281.5	278.8	275.8
$\Delta H_{ice1}/\text{kJ kg}^{-1}$	190.09	189.74	106.38	81.12
$\Delta H_{ice}/\text{kJ kg}^{-1}$	335	335	335	335
$\Delta H_{gas1}/\text{kJ kg}^{-1}$	130.45	128.41	93.78	123.36
$\Delta H_{gas}/\text{kJ kg}^{-1}$	301.57	296.14	137.42	162.77

kJ kg^{-1} , fusion heat shown for ice in the figures; and $\Delta H_{ice}/\text{kJ kg}^{-1}$, standard value of fusion heat, 335.

Table 1 shows the thermal property of single gas hydrate.

With regard to the HCFC-141b hydrate, the thermal properties are (281.2 K, $301.57 \text{ kJ kg}^{-1}$) and (281.5 K, $296.14 \text{ kJ kg}^{-1}$) for two samples; the standard value of thermal property for HCFC-141b hydrate is (281.48 K, 344 kJ kg^{-1}) [47]. That is to say, the deviation for temperature is only 0.28 and 0.02 K, and the recorded temperature is more close to the standard value than another tested temperature (279.65 K) with DSC by previous researcher [34]. Also, the deviation rate for fusion heat is about 13%; obviously, the apparatus is reliable for thermal analysis with DSC for hydrates. Also, we can see, with regard to this DSC device, that it is more accurate for temperature than heat tests in the melting process for sample.

With regard to the TBAB hydrate, the thermal property is (278.8 K, $137.42 \text{ kJ kg}^{-1}$). Since TBAB and water are soluble with each other in the hydrate formation different from HCFC-141b and water, different thermal properties (i.e., temperature and fusion heat) have been shown based

on phase-change temperature which is lower than the critical decomposition temperature point (285.15 K) in the standard phase equilibrium diagram [48].

With regard to the THF hydrate (275.8 K, 162.77 kJ kg⁻¹), since THF and water are also mutually soluble, it is also easily explained by the fact that the phase-change temperature is lower than the critical decomposition temperature point (277.55 K) in the standard phase equilibrium diagram [47].

The thermal properties of TBAB hydrate and THF hydrate provide the basis for the potential application in air conditioning for cold storage. It can also be seen that TBAB hydrate usually has the superiority in phase-change temperature while THF hydrate usually has more advantage in fusion heat for cold storage when compared with each other.

DSC curves of TBAB-THF hydrate

The DSC curves of TBAB-THF mixture hydrate are shown in Figs. 9 and 10. Three melting endothermic peaks in the reversing heat flow curve can be observed in these figures for three substances (ice, TBAB, and THF). The first is for ice, second for THF hydrate, and third is for TBAB hydrate.

The average phase-change temperature (t_m) for TBAB-THF mixture hydrate is deduced as follows:

$$\begin{aligned} t_m &= (t_{\text{THF}} \times m_{\text{THF}} + t_{\text{TBAB}} \times m_{\text{TBAB}}) / (m_{\text{THF}} + m_{\text{TBAB}}) \\ &= [t_{\text{THF}} \times (m_{\text{THF}}/m_{\text{TBAB}}) + t_{\text{TBAB}}] / (m_{\text{THF}}/m_{\text{TBAB}} + 1) \end{aligned} \quad (2)$$

where t_{THF}/K is phase-change temperature for THF hydrate; t_{TBAB}/K , phase-change temperature for TBAB hydrate; m_{THF}/g , mass for THF hydrate; and m_{TBAB}/g , mass for TBAB hydrate.

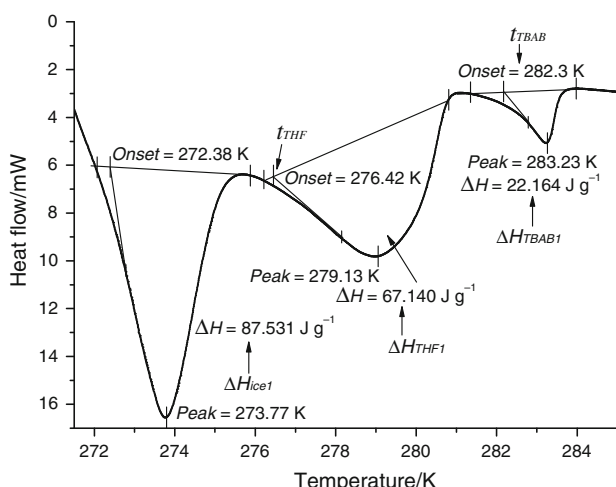


Fig. 9 DSC melting curve of TBAB-THF hydrates (1)

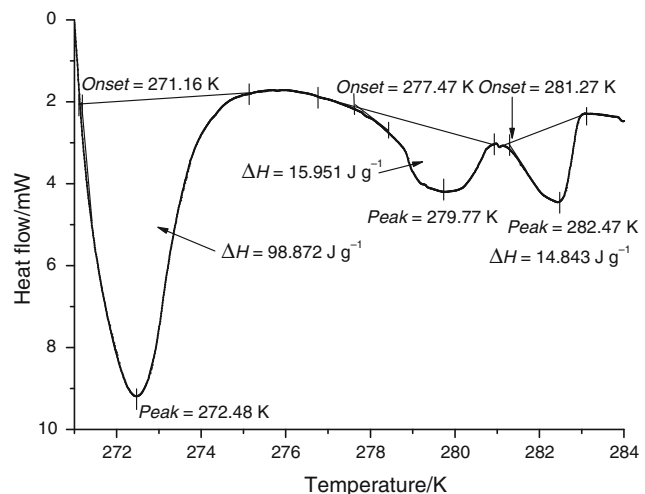


Fig. 10 DSC melting curve of TBAB-THF hydrates (2)

$$\begin{aligned} m_{\text{THF}}/m_{\text{TBAB}} &= (n_{\text{THF}} \times M_{\text{THF}})/(n_{\text{TBAB}} \times M_{\text{TBAB}}) \\ &= 0.6017 n_{\text{THF}}/n_{\text{TBAB}} \end{aligned} \quad (3)$$

From Figs. 9 and 10, it can be seen that excessive ice existed in the sample, since TBAB hydrate and THF hydrate have both types of hydrate structures [14]; their molecular formula usually are TBAB·17H₂O and THF·17H₂O, respectively. Thus, $M_{\text{THF}}/\text{g mol}^{-1}$ is molar mass for THF hydrate, 378.1 and $M_{\text{TBAB}}/\text{g mol}^{-1}$ is molar mass for TBAB hydrate, 628.37. To $n_{\text{THF}}/n_{\text{TBAB}}$, the mole ratios of THF hydrate and TBAB hydrate can be easily drawn from the part of sample preparation in this article that the values for TBAB-THF hydrate are 9.00 and 2.33 for samples (1) and (2), respectively.

From Eqs. 4 and 5, t_m can be easily induced as follows:

$$t_m = [0.6017 t_{\text{THF}} \times (n_{\text{THF}}/n_{\text{TBAB}}) + t_{\text{TBAB}}] / (0.6017 n_{\text{THF}}/n_{\text{TBAB}} + 1). \quad (4)$$

The nominal fusion heat for TBAB-THF hydrate $\Delta H_{\text{TBAB-THF1}}$ is induced as follows:

$$\begin{aligned} \Delta H_{\text{TBAB-THF1}} &= (\Delta H_{\text{THF1}} \times m_{\text{THF}} + \Delta H_{\text{TBAB1}} \times m_{\text{TBAB}}) / (m_{\text{THF}} + m_{\text{TBAB}}) \\ &= [0.6017 \Delta H_{\text{THF1}} \times (n_{\text{THF}}/n_{\text{TBAB}}) + \Delta H_{\text{TBAB1}}] / (0.6017 n_{\text{THF}}/n_{\text{TBAB}} + 1) \end{aligned} \quad (5)$$

Further, the real fusion heat for TBAB-THF hydrate $\Delta H_{\text{TBAB-THF}}$ is deduced as follows:

$$\Delta H_{\text{TBAB-THF}} = \Delta H_{\text{TBAB-THF1}} / (1 - \Delta H_{\text{ice1}}/\Delta H_{\text{ice}}) \quad (6)$$

Table 2 shows the analysis of the thermal property of hydrate mixture. The thermal properties for hydrate mixture are (277.3 K, 81.40 kJ kg⁻¹) and (279.1 K, 21.98 kJ kg⁻¹). The value of $\Delta H_{\text{TBAB-THF}}$ was much lower since lots of ice were produced in the sample; after all, the high-quality of hydrate, especially for hydrate,

Table 2 Analysis of the thermal property of binary gas hydrates

Sample	TBAB–THF hydrate (1)	TBAB–THF hydrate (2)
$m_{\text{total}}/\text{mg}$	22.73	13.94
t_{THF}/K	276.4	277.5
t_{TBAB}/K	282.3	281.3
$n_{\text{THF}}/n_{\text{TBAB}}$	9.00	2.33
t_m/K	277.3	279.1
$\Delta H_{\text{ice}1}/\text{kJ kg}^{-1}$	87.53	98.87
$\Delta H_{\text{ice}}/\text{kJ kg}^{-1}$	335	335
$\Delta H_{\text{THF}1}/\text{kJ kg}^{-1}$	67.14	15.95
$\Delta H_{\text{TBAB}1}/\text{kJ kg}^{-1}$	22.16	14.84
$\Delta H_{\text{TBAB–THF}1}/\text{kJ kg}^{-1}$	60.13	15.49
$\Delta H_{\text{TBAB–THF}}/\text{kJ kg}^{-1}$	81.40	21.98

mixture is not easily obtained since both weighing and transferring them to DSC instrument took a longer time, which may make part of the samples for dehydrate. As a result, the real part of hydrate in the sample is not a large part, which may not make very desirable results.

In spite of this, more importantly, the results shows that, with the increased component of THF in hydrate mixture, the phase-change temperature for hydrate mixture has been lower, while the fusion heat has increased; which presents a good trend for cold storage in air-conditioning system. Also, the temperatures (277.3 K and 279.1 K) are very close to the range of ideal temperature (278–281 K) for cold storage in air-conditioning system.

It reveals the principle of superiority of binary hydrates to that of singular one from a broader view: adding appropriate amount of hydrate with lower phase-change temperature to hydrate with higher one can make the hydrate mixture more suitable for cold storage; some hydrates with lower phase-change temperature can even make the fusion heat of hydrate mixture increase greatly. Also, the principle has been verified extensively from the view of the growth kinetics and phase-equilibrium properties, such as shorter induction time for hydrate, accelerated formation rate, etc. [49–52]. That is to say, the hydrate mixture has the advantages of both kinds of single hydrates.

In reality, for a cold storage system, the preparation for hydrate is easier than that for DSC (the mass of sample is very small, and it is easy to dehydrate when weighing and transferring, also more ice has been produced during DSC experiment). More seriously, hampered by the deficiencies of higher phase temperature of single hydrate beyond the range for cold storage in air-conditioning system (278–281 K), many potential single hydrates are not very suitable considering the economical feasibility. On the basis of the principle of superiority of binary hydrates, and the

Table 3 New environmental working pairs for binary gas hydrates

Working pairs for binary gas hydrates		
HFC-152a/HFC-365mfc	HFC-152a/HFC-245fa	HFC-152a/HFC-245ca
HFC-152a/THF	HFC-125/THF	HFC-134a/i-C ₄ H ₁₀
HFC-152a/i-C ₄ H ₁₀	HFC-125/i-C ₄ H ₁₀	HFC-152a/C ₅ H ₁₀
HFC-134a/C ₅ H ₁₀	TBAB/HC-290	TBAB/C ₅ H ₁₀
HFC-134a/THF	TBAB/i-C ₄ H ₁₀	TBAB/THF
HFC-125/HFC-365mfc	HFC-125/HFC-245fa	HFC-125/HFC-245ca
HFC-227ca/HFC-245fa	HFC-227ca/HFC-245ca	HFC-227ca/FC-236ea
HFC-134a/HFC-365mfc	HFC-134a/HFC-245fa	HFC-134a/HFC-245ca
HFC-227ea/HFC-365mfc	HFC-227ea/HFC-245fa	HFC-227ea/HFC-245ca
HFC-227ea/HFC-236ea	HFC-227ea/HC-631	HFC-227ca/HFC-365mfc
HFC-134a/HFC-236ea	HFC-134a/HC-631	HFC-152a/HFC-236ea
HFC-152a/HC-631	HFC-125/HFC-236ea	HFC-125/HC-631

properties [47] of single working medium for hydrate formation, possible new environmental-friendly medium pairs for binary hydrates are listed in Table 3.

Conclusions

This study demonstrates the preliminary feasibility of thermodynamics analysis by DSC for mixture hydrate (e.g., TBAB–THF hydrate) for cold storage in air-conditioning system, which presents the perspective that TBAB–THF hydrates are more suitable than single hydrate (TBAB hydrate, THF hydrate) for proper phase-change temperature and increased fusion heat, despite certain discrepancies that have been caused during the process of hydrate formation and DSC experiment.

In this study, one important conclusion is that the binary hydrates have the principle of superiority of to that of singular one from broader view: appropriate amount of hydrate with lower phase-change temperature adding to hydrate with higher one can make the mixture hydrate more suitable for cold storage; some hydrates with lower phase-change temperature can even make the fusion heat of hydrate mixture increase greatly.

The principle has been verified by researchers closely and extensively. In the face of difficulty of limited kinds of hydrate for cold storage in air-conditioning, several new environmental-friendly working pairs for binary gas hydrates have been listed to help to promote the application.

It should be noted that the high-quality of dense sample of hydrate with less ice for DSC is not easy to obtain. More preparation work should be done to ensure the accuracy for DSC tests. In addition, further study is also needed to determine the feasibility of new environmental-friendly binary hydrates in a more broad range of different kinds for cold storage in air-conditioning system by DSC for thermodynamics study.

Acknowledgements This study was partly supported by the National Natural Science Foundation of China (Nos. 50706028 and 50806050), and the Shanghai Leading Academic Discipline Project (No. S30503).

References

1. Borenstein S. The trouble with electricity markets: understanding California's restructuring disaster. *J Econ Perspect*. 2002;16: 191–211.
2. Night breeze cuts peak demand, keeps residents cool (Public Interest Energy Research Program). California Energy Commission; 2009. <http://www.energy.ca.gov>. Accessed 3 Mar 2009.
3. Analysis Report for Electric Power Industry of China in 2009. State Information Center of China; 2009. <http://report.cei.gov.cn>. Accessed 10 Oct 2009.
4. Fan SS, Xie YM, Guo KH, Liang DQ, Gu JM. Advances of gas hydrate cool storage technologies used in air conditioning system. *J Chem Ind Eng*. 2003;54(Suppl):131–5.
5. Ogoishi H, Takao S. Air-conditioning system using clathrate hydrate slurry. *JFE Tech Rep*. 2004;3:1–5.
6. Liang DQ, Wang RZ, Guo KH, Fan SS. Prediction of refrigerant gas hydrates formation conditions. *J Therm Sci*. 2001;10:64–8.
7. Fournaison L, Delahaye A, Chatti I, Petit JP. CO₂ hydrates in refrigeration processes. *Ind Eng Chem Res*. 2004;43:6521–6.
8. Fan SS, Wang JY. Progress of gas hydrate studies in China. *Chin J Process Eng*. 2006;6:997–1003.
9. Marinhos S, Delahaye A, Fournaison L, Dalmazzone D, Fürst W, Petit JP. Modelling of the available latent heat of a CO₂ hydrate slurry in an experimental loop applied to secondary refrigeration. *Chem Eng Process*. 2006;45:184–92.
10. Li JP, Liang DQ, Guo KH, Wang RZ, Fan SS. Formation and dissociation of HCFC134a gas hydrate in nano-copper suspension. *Energy Convers Manag*. 2006;47:201–10.
11. Bi YH, Guo TW, Zhu TY, Zhang L, Chen LG. Influences of additives on the gas hydrate cool storage process in a new gas hydrate cool storage system. *Energy Convers Manag*. 2006;47: 2974–82.
12. Li G, Xie YM, Liu DP. Effects of SDS on formation of new-type cool storage medium-isobutene gas hydrates. *J Chem Ind Eng*. 2008;59:60–3.
13. Davidson DW. Water: a comprehensive treatise. In: Franks F, editor. Clathrate hydrates, vol. 2. New York: Plenum Press; 1973. p. 115–234.
14. Sloan ED, Koh Carolyn. Clathrate hydrates of natural gases, 3rd ed. Boca Raton, FL: CRC Press; 2007. p. 11–14.
15. Khokhar AA, Gudmundsson JS, Sloan ED. Gas storage in structure H hydrates. *Fluid Phase Equilib*. 1998;150–151:383–92.
16. Mori YH. Recent advances in hydrate-based technologies for natural gas storage—a review. *J Chem Indus Eng*. 2003;54(Suppl):1–17.
17. Hao WF, Wang JQ, Fan SS, Hao WB. Evaluation and analysis method for natural gas hydrate storage and transportation processes. *Energy Convers Manag*. 2008;49:2546–53.
18. Dong F, Lou HM, Kodama A, Goto M, Hirose T. The Petlyuk PSA process for the separation of ternary gas mixtures: exemplification by separating a mixture of CO₂–CH₄–N₂. *Sep Purif Technol*. 1999;16:159–66.
19. Ebinuma T. Method for dumping and disposing of carbon dioxide gas and apparatus therefore. US Patent 5,261,490; 1993.
20. Linga P, Kumar RN, Englezos P. Gas hydrate formation from hydrogen/carbon dioxide and nitrogen/carbon dioxide gas mixtures. *Chem Eng Sci*. 2007;62:4268–76.
21. Zhou XT, Fan SS, Liang DQ, Du JW. Determination of appropriate condition on replacing methane from hydrate with carbon dioxide. *Energy Convers Manag*. 2008;49:2124–9.
22. Yang HQ, Xu ZH, Fan MH, Gupta R, Slimane RB, Bland AE, Wright I. Progress in carbon dioxide separation and capture: a review. *J Environ Sci*. 2008;20:14–27.
23. Chatti I, Delahaye A, Fournaison L, Petit JP. Benefits and drawbacks of clathrate hydrates: a review of their areas of interest. *Energy Convers Manag*. 2005;46:1333–43.
24. Cantor S. Applications of DSC (differential scanning calorimetry) to the study of thermal energy storage. *Thermochim Acta*. 1978;26:39–46.
25. Rueff RM, Sloan ED, Yesavage VF. Heat capacity and heat of dissociation of methane hydrates. *AIChE J*. 2004;34:1468–76.
26. Le Parlouer P, Christine Dalmazzone, Herhaft B, Rousseau L, Mathonat C. Characterisation of gas hydrates formation using a new high pressure Micro-DSC. *J Therm Anal Calorim*. 2004;78: 165–72.
27. Giavarini C, Maccioni F, Santarelli ML. Modulated DSC for gas hydrates analysis. *J Therm Anal Calorim*. 2006;84:419–24.
28. Gupta A, Lachance J, Sloan ED, Koh CA. Measurements of methane hydrate heat of dissociation using high pressure differential scanning calorimetry. *Chem Eng Sci*. 2008;63:5848–53.
29. U.S. Environmental Protection Agency. <http://www.epa.gov/Ozone/intpol/>.
30. Rueff R M, Sloan ED, Yesavage VF. Heat capacity and heat of dissociation of methane hydrates. *AIChE J*. 1988;34:1468–76.
31. Loevois JS, Perkins R, Martin RJ. Development of an automated, high pressure heat flux calorimeter and its application to measure the heat of dissociation and hydrate number of methane hydrate. *Fluid Phase Equilib*. 1990;59:73–9.
32. Handa YP. Compositions enthalpies of dissociation, and heat capacities in the range 85 to 270 K for clathrate hydrates of CH₄, C₂H₆, C₃H₈. *J Chem Therm*. 1986;18:15–21.
33. Handa YP. Calorimetric determinations of compositions, enthalpies of dissociation, and heat capacities in the range 85 to 270 K for clathrate hydrates of xenon and krypton. *J Chem Therm*. 1986;18:891–5.
34. Liang DQ, Guo KH, Fan SS, Wang RZ. Measurement of melting heat of HCFC-141b gas hydrate with DSC. *J Eng Thermophys*. 2002;23:47–9.
35. Deschamps J, Dalmazzone D. Dissociation enthalpies and phase equilibrium for TBAB semi-clathrate hydrates of N₂, CO₂, N₂ + CO₂ and CH₄ + CO₂. *J Therm Anal Calorim*. 2009;98: 113–8.
36. Dalmazzone D, Kharrat M, Lachet V, Fouconnier B, Clausse D. DSC and PVT measurements: Methane and trichlorofluoromethane hydrate dissociation equilibria. *J Therm Anal Calorim*. 2002;70:493–505.
37. Chen J, Ma P, Chen G, Chen F. The measurement of hydration heats for magnesium chloride with low water by means of DSC. *J Therm Anal Calorim*. 2001;65:777–86.
38. Berbenni V, Milanese C, Bruni G, Marini A. Thermal decomposition of gallium nitrate hydrate Ga(NO₃)₃ × H₂O. *J Therm Anal Calorim*. 2005;82:401–7.
39. Kimura A, Miyake A, Ogawa T. Thermal properties of hydrazine in nitric acid solution. *J Therm Anal Calorim*. 2008;93:35–9.

40. Komunjer L, Ollivon M, Fouconnier B, Luong AT, Pezron I, Clausse D. Influence of sodium chloride on the melting of ice and crystallization and dissociation of CCl_3F hydrate in water in oil emulsion. *J Therm Anal Calorim*. 2009;98:125–31.
41. Lipkowski J, Komarov VY, Rodionova TV, Dyadin YA, Aladko LS. The structure of tetrabutylammonium bromide hydrate ($\text{C}_4\text{H}_9)_4\text{NBr}_2^{1/3}\text{H}_2\text{O}$. *J Supramol Chem*. 2002;2:435–9.
42. Oyama H, Shimada W, Ebinuma T, Kamata Y, Takeya S, Uchida T, Nagao J, Narita H. Phase diagram, latent heat, and specific heat of TBAB semiclathrate hydrate crystals. *Fluid Phase Equil*. 2005;234:131–5.
43. Shimada W, Ebinuma T, Oyama H, Kamata Y, Narita H. Free-growth forms and growth kinetics of tetra-*n*-butyl ammonium bromide semi-clathrate hydrate crystals. *J Cryst Growth*. 2005;274:246–50.
44. Darbouret M, Cournil M, Herri JM. Rheological study of TBAB hydrate slurries as secondary two-phase refrigerants. *Int J Refrig*. 2005;28:663–71.
45. Rodionova TV, Manakov AY, Stenin YG, Villevaud GV, Karpova TD. The heats of fusion of tetrabutylammonium fluoride ionic clathrate hydrates. *J Incl Phenom Macrocycl Chem*. 2008;61:107–11.
46. American Chemical Society (CAS) Databases. <http://www.cas.org/expertise/cascontent/index.html>.
47. Guangzhou Institute of Energy Conversion, CAS. New Energy Source & Environmental Protection Database. http://www.newenergy.csdb.cn/index_en.asp.
48. Fan SS. Natural gas hydrate storage and transportation technology. Beijing: Chemical Industry Press; 2005.
49. Guo KH, Zhang Y, Shu BF. Study on phase-equilibrium property of HFC152a/HCFC141b mixed gas hydrate. *J Eng Thermophys*. 1997;18:657–60.
50. Guo KH, Shu BF, Zhang Y, Zhao YL. Phase-equilibrium property of HFC134a/HCFC141b mixed gas hydrate. *J Eng Thermophys*. 1998;19(4):480–3.
51. Li JP, Wu J, Liang DQ, Guo KH, Wang RZ, Qi XY. Experimental study on formation process of gas hydrate in nanofluids. *J Xi'an Jiao Tong Univ*. 2006;40:365–8.
52. Liu Y, Guo KH, Liang DQ, Fan SS, Zhao YL. Mixed refrigerant hydrate formation and decomposition process. *J Harbin Inst Technol*. 2004;36:242–5.